# Toward an Integrated Biomimetic Model of Reaching

Daniele Caligiore, Domenico Parisi and Gianluca Baldassarre
*Laboratory of Autonomous Robotics and Artificial Life,*
*Istituto di Scienze e Tecnologie della Cognizione, Consiglio Nazionale delle Ricerche (LARAL-ISTC-CNR)*
*Via San Martino della Battaglia 44, I-00185 Roma, Italy*
{*daniele.caligiore, domenico.parisi, gianluca.baldassarre*}*@istc.cnr.it*

***Abstract*— One of the most influential principles of motor development theory, the circular-reaction hypothesis, states that infants perform exploratory movements to acquire efferent-reafferent associations later used to perform goal directed behavior. All models proposed so far to specify this principle lack biological plausibility under some respects. This work proposes a model that starts to overcome these limitations. In particular, the model aims to show that overcoming such limitations in an *integrated fashion* can shed new light on so-far overlooked phenomena of motor development. This goal is pursed by showing how the model develops biologically plausible connections and movement smoothing mechanisms as *emergent outcomes* of the interplay between its various biologically-plausible features: a dynamic arm with realistic parameters, an equilibrium-point muscle model, a leaky-neuron neural controller based on population codes, and a Hebb learning rule.**

***Index Terms*— Sensorimotor coordination, reaching, Hebb, motor babbling, equilibrium point, EP, muscle, dynamic arm.**

## I. Introduction

Children's acquisition of skills on the basis of *circular reactions* [1] is one of the most influential principles proposed by theories of motor development . For example, it has been proposed [2] that infants learn eye-hand coordination on the basis of the production of (often random) movements (*motor babbling*) that enhance the association between efferent motor patterns and re-afferent perceptive patterns.

Several neural-network models have been proposed with the aim of detailing at a neural level the functioning of the circular-reaction principle (e.g. [3], [4], [5], [6], [7], [8]). Notwithstanding the great relevance of these contributions, all the proposed models are limited with respect to one or more aspects of biological plausibility. The first limitation is the use of simplified kinematic arms to simulate the motor system (e.g. [3], [4], [6]): this simplifies learning (e.g. due to the absence of inertia) but leads to overlook the problem of dynamic stability. The second limitation is the use of a simplified muscle model (e.g. [3], [5], [6]). This can lead to miss the opportunity of having stabilizing mechanisms "for free", and in general control problems different from those faced by real organisms (cf. [9], [10]). The third limitation is the use of supervised learning algorithms (e.g. [3], [5], [6]). These algorithms are computationally very powerful but require the strong assumption that each neuron receives a dedicated teaching signal: with few exception (e.g. the cerebellum) this assumption is not supported by empirical evidence. The fourth limitation is the use of firing-rate neurons (e.g. sigmoid neurons) with no internal dynamics as those characterizing real neurons (e.g. [3], [4], [5], [6], [7], [8]). The last limitation is the absence of neuroscientific evidence supporting the overall systems' architecture and sensory/motor pattern encoding (e.g. [3], [6]).

This work represents a first step toward building a model of development of reaching skills based on motor babbling that overcomes the aforementioned limitations. First, the model proposed uses a dynamic arm model with human arm parameters [11]. Second, it uses the $\lambda$ muscle model [12], [10] based on the *Equilibrium Point Hypothesis*, one of the most accredited theories of motor organization, that offers interesting solutions to the problems of motor redundancy [13] and stability [9]. Third, the model uses a "canonic" covariance Hebb's rule [14] to develop sensorimotor skills with motor babbling. Fourth, the model's controller is formed by leaky neuron maps [15]: although less accurate than spike neurons, these neurons have been preferred to the latter as more simple but still reproducing some dynamical properties of real neurons [15]. Last, the model's architecture incorporates important neuroscientific evidence suggesting that: (a) parietal cortex plays an important role for eye-hand coordination as it encodes target locations, as final stage of visual neural pathways [16], and postures, as final stage of proprioception pathways [17]; (b) premotor cortex encodes motion on the basis of limbs' desired end postures [18]; (c) many sensory and motor variables in the brain are encoded by the activity of large populations of neurons, having broad tuning curves, by exploiting their spatial location in brain space (*population code hypothesis*, [19]; e.g. see [20]).

At first sight, this list might seem to lead to a model that merely juxtaposes interesting biologically-plausible mechanisms. On the contrary, one of the major goals of the paper is to show that the *integration* of such aspects can produce insights on so-far overlooked phenomena related to organisms' brain and behavior systemic functioning. The paper presents three results that support this claim. First, the model presented shows that, thanks to its architecture and the

This research was supported by the EU Projects *ICEA*, contract no. FP6-IST-027819-IP, and *MindRACES*, contract no. FP6-511931-STREP.

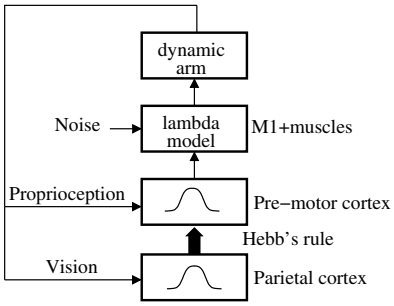


Fig. 1. The architecture of the system, formed by a neural controller, a $\lambda$ muscle model, and a dynamic arm model. The graph also indicates the system brain areas corresponding to the different parts of the architecture. Arrows refer to information flows, while the bold arrow represents connection weights trained on the basis of an Hebb rule (see text for details). The two Gaussian curves in the cortex maps hint to the fact that they use population code representations of sensorimotor information.

population codes, a simple covariance Hebb rule and motor babbling are sufficient to produce the development of quite accurate reaching skills. Second, the use of leaky neurons, a dynamic arm, and the covariance Hebb rule produces a high contrast representation of targets based on the emergence of connection weights having a Mexican hat distribution [21]. Third, the use of leaky neurons and re-afferent proprioception allows obtaining a stabilization of the motion of the dynamic arm, and a joints' angular speed with a typical bell shape as the one observed in experiments with humans [22].

In the remaining part of the paper, Sect. II presents the dynamic arm, the muscle model, and the neural-network architecture, Sect. III presents the results, Sect. IV discusses the relevance of the results and the limitations of the model.

## II. Methods

Fig. 1 shows the components of the model: a neural controller that issues desired arm postures (EPs) to a $\lambda$ model which computes muscle torques to be sent to a dynamic arm model. The controller was a neural network with two layers encoding respectively the hand or target position, encoded as points in extrinsic space coordinates, and the arm's desired posture, encoded as a point in posture space. These two layers were assumed to encode respectively late-stage visual representations of stimuli at the level of parietal cortex, and arm movements planned in terms of desired final postures (EPs) at the level of pre-motor cortex. In a first phase of life the system performed random movements to learn, with a covariance Hebb rule, the association between visually perceived hand's positions and corresponding postures.

### A. Muscle Model

The arm, assumed to work on the plane, was formed by an upper and lower segment respectively measuring $30cm$ and $40cm$. Each segment was controlled by a couple of flexor/extensor muscles acting at the shoulder and elbow joints. According to equilibrium point hypothesis [12], every muscle is controlled by a parameter $\lambda$ specified by the central nervous system. The $\lambda$s of each couple of extensor/flexor muscles are used to generate two opposing torques, $T_e$ and $T_f$, as follows:

$$\begin{aligned} T_e &= \rho h(\exp(\alpha[\lambda_e - q - \mu\dot{q}]^+) - 1) \\ T_f &= \rho h(\exp(\alpha[-\lambda_f + q + \mu\dot{q}]^+) - 1) \end{aligned} \quad (1)$$

where $q$ is the joint angle (in radiants), $\dot{q}$ is its first derivative (angular speed), $\lambda$ is the static threshold of motoneuronal recruitment, $\mu$ the coefficient of the reflex damping torque, $\rho$ is the strength of the muscle, $h$ is the muscle moment arm, and $\alpha$ is a function-form parameter. $\tilde{\lambda} = \lambda - \mu\dot{q}$ is the dynamic threshold of motoneuronal recruitment. When $q > \tilde{\lambda}$, the muscle produces a torque with a level that is an increasing function of $[\tilde{\lambda} - q]^+$. The torques from equation (1) are filtered by a second-order low-pass filter to mimic the gradual muscle activation due to calcium-dependent processes:

$$M_k + \tau_1\dot{M}_k + \tau_2^2\ddot{M}_k = T_k \quad (2)$$

where k refers to either the extensor or flexor muscle, $M$ is the muscle torque that gradually reaches the steady-state value $T$, and $\tau_1$ and $\tau_2$ are the time constants of the filter. The dependence of the muscle force on the sliding of muscle filaments is accounted for with a linearized version of Hill's relationship [23], $n_k = M_k(1 + a\dot{q})$, where $n$ is the torque and $a$ the intrinsic muscle damping. Finally, the net torque acting on a single joint is computed as $T = n_e - n_f$. The neural controller issues the EPs related to the shoulder and elbow to the $\lambda$ model through two parameters, $R_{shoulder}$ and $R_{elbow}$. These parameters determine the couple of $\lambda$ values for each joint on the basis of the following equations:

$$\lambda_e = R + C, \quad \lambda_f = R - C \quad (3)$$

where $C$ is a further variable corresponding to different levels of co-activation (stiffness) of antagonist muscles. Generally it is assumed that the nervous system regulates the $C$s and $R$s independently, so, given the scope of this work, the $C$s were set to constant values.

All the parameters of the $\lambda$ model were set to the same values used in [10], obtained with physiological measurements, with the exception of $\mu$, $\tau_1$ and $C$s (shoulder and elbow). $\mu$ was set to $0.3s$ vs. an original value of $0.075s$. The reason was that in [10] EPs were gradually changed, so a small $\mu$ was sufficient to guarantee the necessary stabilizing damping effect (see equation (1)). On the contrary, in some experiments reported here the EPs (and hence the $\lambda_e - q$ and the related torques) change quite abruptly, so a higher $\mu$ allowed having a higher stabilizing damping effect. This also causes torques to reach high values with respect to [10] and so $\tau_1$ was set to $0.12s$ vs. the original $0.02s$. Finally,

$C$s were set to $3.0Nm/rad$ vs. the original $2.0Nm/rad$ as here only two couple of antagonist muscles were used vs. the three couples used in [10].

### B. Dynamic Arm Model

The system used a dynamical human arm model having the realistic bio-mechanical parameters proposed in [11]. The ranges of variation of the shoulder and elbow joint angles were respectively $0/3.14rad$ and $0/2.8rad$. The torques values obtained from the $\lambda$ model were used by the dynamic arm model to obtain the angular position, the angular speed and the angular acceleration of the arm segments using standard Lagrangian formulations [24]:

$$\mathbf{B}(\mathbf{q})\ddot{\mathbf{q}} + \mathbf{C}(\mathbf{q},\dot{\mathbf{q}})\dot{\mathbf{q}} + \mathbf{D}(\dot{\mathbf{q}}) + \mathbf{g}(\mathbf{q}) = \mathbf{T} \tag{4}$$

where $\mathbf{q} = [\alpha, \beta]$ is the vector of the angles, $\dot{\mathbf{q}} = [\dot{\alpha}, \dot{\beta}]$ the vector the angular speeds, $\ddot{\mathbf{q}} = [\ddot{\alpha}, \ddot{\beta}]$ the vector of the accelerations of the shoulder/elbow joints, $\mathbf{B}(\mathbf{q})$ the inertia matrix, $\mathbf{C}(\mathbf{q},\dot{\mathbf{q}})$ the matrix accounting for Coriolis and centrifugal effects, $\mathbf{D}(\dot{\mathbf{q}})$ the matrix related to friction (here assumed to be null), $\mathbf{g}(\mathbf{q})$ the torque due to gravity (here null), $\mathbf{T}$ the total torques applied to the joints.

### C. Neural Controller and Learning Procedure

The neural controller was formed by two 2D maps of $21 \times 21$ neurons. The units of the two maps were assumed to occupy positions on the vertexes of a regular 2D lattice in the brain space. The *parietal cortex* map received, as visual input, the position of hand (end-effector of simulated arm), or position of target objects, expressed in extrinsic space x-y coordinates. The *pre-motor cortex* map received, as proprioceptive input, the arm posture expressed in intrinsic space joint angles. The pre-motor cortex also received input signals from the parietal cortex via all-to-all connections trained with a Hebb rule, and its activation was "read out" to produce the $R$s values for the $\lambda$ model (see below).

The neurons forming the two maps were leaky neurons [15] having an activation $a[j,t]$ and an activation potential $u[j,t]$ at time $t$ with the following dynamics:

$$\begin{aligned} a[j,t] &= f[u[j,t]] \\ u[j,t+\triangle t] &= \\ = \left(1 - \frac{\Delta t}{\tau}\right) u[j,t] &+ \frac{\Delta t}{\tau}\left(S[j,t] + h + \sum_{i=1}^{N} w_{ji} a[i,t]\right) \end{aligned} \tag{5}$$

where $\Delta t = 0.01s$ was the integration time step (100 steps corresponded to $1s$), $S[x,t]$ the input pattern, $\tau = 0.3s$ the relaxation time, $h$ the neuron equilibrium value (here set to zero), and $f$ a $[tanh[.]]^+$ activation function. In the case of the pre-motor cortex, the sum of the formula accounted for the signals $a[i,t]$ received from all the neurons of the parietal cortex modulated by the respective connection weights $w_{ji}$.

For both maps, the activation of neurons due to the external sensory signal was generated on the basis of a Gaussian function capturing the assumption that stimuli (hand, object or posture) with coordinates close to the *preferred coordinates* of neurons cause a high activation of them, whereas farther stimuli cause progressively lower activations:

$$S[j] = f[\mathbf{x}, \mathbf{x_j}] = \exp\left(-\frac{|\mathbf{x} - \mathbf{x_j}|}{2\sigma^2}\right) \tag{6}$$

where $\mathbf{x}$ were the coordinates of the stimulus and $\mathbf{x_j}$ the preferred coordinates of the neuron (in order to compute the dimensions of $\mathbf{x}$ and $\mathbf{x_j}$, the whole range of each coordinate was mapped onto the "brain space" situated between the third and the nineteenth neuron along one dimension of the map).

To obtain the two EPs for the arm, it was assumed that the activations $a[j,t]$ of the pre-motor cortex neurons encoded them in terms of a *population code* "read out" as follows [19]:

$$\mathbf{R} = \frac{\sum_{j=1}^{N} \mathbf{x_j} a[j]}{\sum_{j=1}^{N} a[j]} \tag{7}$$

where $\mathbf{R}$ was the shoulder/elbow joints' EPs vector.

As mentioned, the system's life was divided in two phases: (1) a "childhood" phase where it learned a mapping between the visual stimulus generated by its own hand (parietal cortex) and the corresponding posture (pre-motor cortex) on the basis of random movements and a Hebbian learning rule; (2) an "adult" phase in which it used the knowledge so acquired to accomplish reaching movements to targets.

During the childhood phase, that lasted 30 minutes (180,000 cycles), the system performed motor babbling: setting different random $R$s for the $\lambda$ model, were external generated every 0.5 sec (50 cycles). The visual stimulus of the hand and the proprioceptive stimulus of the posture were used to respectively activate the parietal cortex and the pre-motor cortex according to equation (6). The weights of the connections between all couples $(a_j, a_i)$ of parietal cortex and pre-motor cortex neurons were updated according to the following *covariance Hebb rule* [14]:

$$\Delta w_{ji} = \eta(a_j - \overline{a}_j)(a_i - \overline{a}_i)(w_{max} - |w_{ji}|) \tag{8}$$

where $\eta$ was the learning rate set to 12, and $w_{max}$, set to 0.2, was a parameter that kept the weights within the range of $[-0.2, 0.2]$, $\overline{a}_j$ and $\overline{a}_i$ were moving decaying averages of the neurons' activations, calculated as $\overline{a} = \xi\overline{a} + (1-\xi)a$ with $\xi$ set to 0.2. This rule strengthened the connections between each couple of neurons that had both an activation above average or below average, whereas it weakened the connections in the other cases. As we will see, the effect of this rule was to form an association between the hand's visual perception and the corresponding posture's proprioception.

In the adult phase the system saw a target object but not its own hand (this filtering was assumed to be the result of an attentional mechanism). The perception of the object

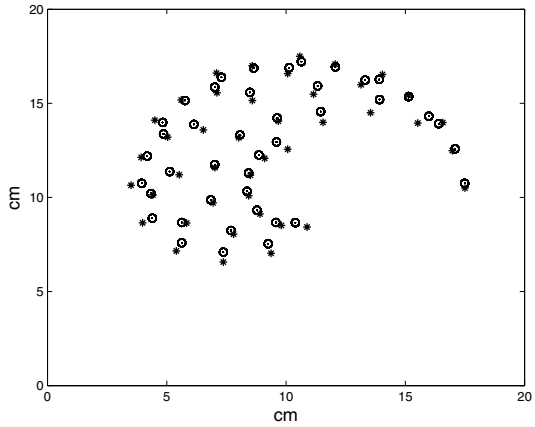


Fig. 2. System's reaching ability acquired with motor babbling. Stars represent 42 target positions and circles represent the final positions of hand at the end of reaching movements lasting $10s$ each. For each target, the system accomplished 42 reaching actions starting from the positions marked by the same stars, for a total of $42 \times 42$ actions (only 42 circles appear in the graph as the hand reached the same final position for each target).

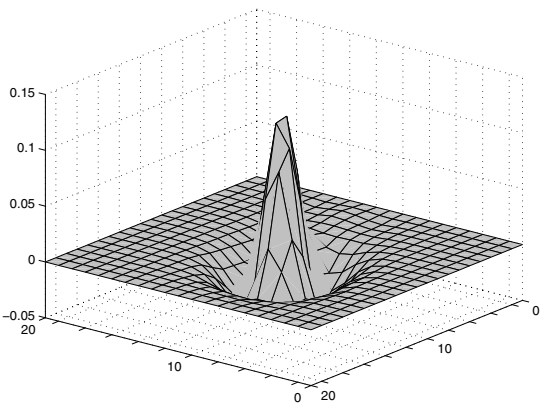

Fig. 3. Activation potential (z-axis) of the pre-motor cortex neurons (xy-plane) when the parietal cortex is activated by an object and proprioception is gated out. The outward weights of each parietal cortex neuron have a similar configuration (data not shown).

caused an activation of the parietal cortex that on its turn caused, via the Hebb-trained connections, the activation of the representation of a posture corresponding to an hand position located on the target. This activation caused a reading out of the pre-motor cortex producing EPs suitable to generate, via the $\lambda$ model, joint torques that drove the hand toward the target. As we will see in Sect. III, two different conditions were used to test the model in the adult phase: one in which the proprioception used during the childhood phase to train the system continued to be present, and one where it was absent on the basis of the assumption that an *internal attentional mechanism* gates it out when the system has terminated the acquisition of the motor skills.

## III. Results

This section presents three results that support the claim that the integration in the same model of various constraints suggested by empirical evidence can lead to discover so-far overlooked phenomena.

### A. Reaching Ability Produced by Motor Babbling and Hebb

Thanks to its architecture and the population codes, the model is capable of developing a satisfying reaching ability on the basis of the simple Hebb rule of equation (8) and the motor babbling process (Fig. 2). Fig. 2 shows that the end position of the hand when the arm reaches 42 different targets is very close to the targets' position, $0.32cm$ on average.

The use of the Hebb rule highlighted the fact that the arm proprioception, that plays an important role during learning, can have important effects on the arm performance. Indeed, other models of motor babbling using supervised learning rule overlooked the fact that the proprioceptive"teaching input" used during training cannot suddenly disappear during functioning unless one assumes the presence of an *attentional mechanism* gating it out. The performance reported in (Fig. 2) has been obtained with this assumption. Interestingly, if this assumption is removed, and proprioception is present after learning, performance drops from $0.32cm$ to $0.57cm$. The reason of this deterioration, illustrated in detail in Subsect. III-C, is that proprioception slows down the movement of the arm.

### B. Analysis of Emerged Weights: Mexican Hat

Fig. 3 shows the weights of the connections between parietal and pre-motor cortex emerged with learning: the values of the outward weights of the parietal cortex have assumed a Mexican hat distribution. To show the reason of this, the following test was run. A row of neurons along one of the two dimensions of the pre-motor cortex map were "artificially" activated with 1 in sequence starting from one end of the row and going toward the neuron at the center of the map: when the map's central neuron was activated the $a_j$ and $\overline{a}_j$ of the whole row of neurons was recorded (Fig. 4a). This activation mimics the activation of neurons in ecological conditions while the dynamic arm *progressively* moves toward a target due to its inertia and muscle damping coefficients. The same measurement was carried out activating the same row of neurons, but this time starting from the neuron at the other end of the row (Fig. 4b). Fig. 4a-b show that these types of dynamical activations of neurons cause the activation $a_j$ of the most activated neuron (the central neuron currently activated by the target) to be higher than its average activation

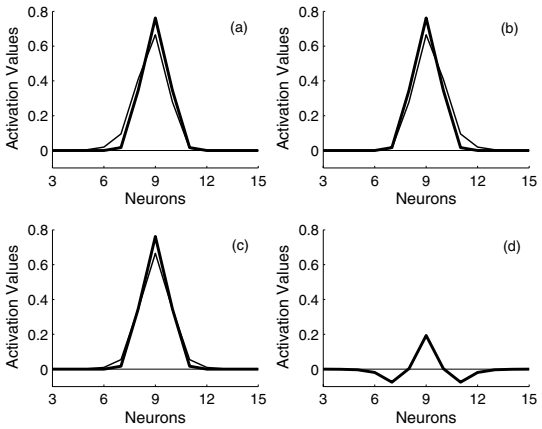


Fig. 4. (a) $a_j$ (bold line) and $\overline{a}_j$ (thin line) of a row of neurons along one dimension of the parietal cortex map (x-axis) when the neurons are activated in sequence from neuron 3 to neuron 9. (b) same measurements when the row of neurons is activated from neuron 15 to neuron 9. (c) averages of the $a_j$ (bold line) and $\overline{a}_j$ (thin line) of the previous two graphs. (d) difference between the average $a_j$ and $\overline{a}_j$ of the previous graph.

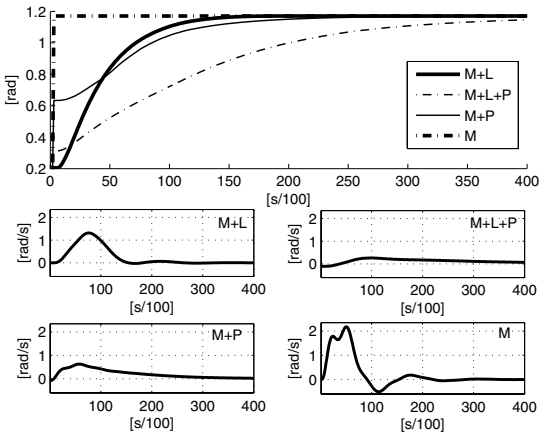


Fig. 5. Top graph: the curves show the dynamics in time (x-axis) of the shoulder's EP when the model performs a reaching movement in four different conditions: with the leaky neurons' relaxation coefficient $\tau = 0.3s$ (M+L), or $\tau = \Delta t = 0.01s$ and without proprioception (M), and the same two conditions with the presence of proprioception (respectively M+L+P and M+P). The four bottom graphs show the angular speed profile of the shoulder joint in the four conditions. The EP and speed profile of the elbow joint, not reported, exhibit similar dynamics.

$\overline{a}_j$ as this average always "chases" $a_j$ with some inertia (delay). For the same reason, at the level of parietal cortex a target appearing in any position cause the corresponding neurons to have a $a_j > \overline{a}_j$. As a consequence of this activations, and the learning rule of equation (8), the weights of the connections between the most activated neurons of premotor cortex corresponding to the current posture, and the neurons of the parietal cortex corresponding to the target, will increase, whereas their neighbors will decrease (the outward connection weights of the off-target parietal cortex neurons will not change as $a_j - \overline{a}_j = 0$). When several of these updates add up (Fig. 4c), the outward weights of the parietal cortex tend to assume a Mexican hat configuration (Fig. 4d).

### C. Analysis of the Dynamical Properties of the Model

This section illustrates the effects of the dynamics of the leaky neurons, and the presence/absence of proprioception, on the dynamics of the movements performed by the model. Four reaching tests were run in four different conditions obtained by combining two manipulations: (a) the relaxation time of the leaky neurons set as done so far, $\tau = 0.3s$, or set to have zero-inertia standard sigmoid neurons, $\tau = \Delta t = 0.01s$; (b) the presence or absence of proprioception (as mentioned in sect. III-A, this can be assumed to be the effect of an internal attention process). During these tests, the EPs and angular speed profiles of shoulder and elbow were recorded. The results of the four tests, reported in Fig. 5 and labeled as M, M+L, M+P and M+L+P, indicate several interesting facts: (a) M leads to unstable movements as the EPs suddenly jump to their final position; (b) M+P gives some stability to the system because the EPs slowly approach their final position after an initial jump; (c) M+L gives the most stable movements, plus speed profiles that closely resembles those of human subjects [22]: the reason is that the EPs move progressively from the initial to the final position without jumps: this is the effect of the inertia of the leaky neurons which loose the activation related to the old target and acquire that of the new one in a progressive fashion; (d) M+L+P gives stable movements but at the cost of a remarkable slowness, due to the fact that proprioception 'attracts' the equilibrium point towards current postures. Overall, these results suggest that the dynamics of the leaky neurons might play an important smoothing and stabilizing effect on movements, and that the presence of an internal attention mechanism gating out proprioception after learning might play an important role in motor performance.

## IV. Discussion and Future Work

This paper presented a model of the development of reaching skills based on motor babbling. The model, the first step of a broader research agenda, integrated various components with remarkable biological plausibility: a dynamic arm with realistic parameters, a $\lambda$ model of muscles, population-code neural representations, a Hebb learning rule. The goal of this exercise was to show that attempts as the one reported here to *integrate* all these aspects can lead to understanding aspects of motor development that have been overlooked by previous models as they focused only on few aspects.

To achieve the goal, the paper presented three major results obtained with the integrated model. First, it showed that the model's architecture and population codes allowed it to acquire reaching skills on the basis of motor babbling and a simple Hebb rule: to the best of the authors' knowledge, this is a novel result. Second, it showed how the progressive movements produced by the dynamic arm, the $\lambda$ model, the dynamics of the leaky neurons, and the covariance Hebb rule led the system to develop high-contrast weights with a Mexican hat distribution. This distribution has been found in several parts of the brain and has been shown to produce important emergent phenomena in neural network models [15], [21], [25]. The result is relevant as this weight distribution was obtained as an emergent property of the nature and the interplay of the different components of the model, contrary to the latter works where it was hardwired. Third, the paper showed that the dynamics of the leaky neurons (or proprioception) can yield (a) stabilization effects on arm's movements by producing progressive shifts of the joints' equilibrium points, and (b) a bell-shaped profile of the joints' speed similar to that observed in human subjects. This result is relevant as in the literature of motor development there seem to be a trend for which these effects tend to be obtained with progressively "more hardwired" mechanisms (e.g. in [10] and [26] EPs are shifted linearly; [27] proposes a neural mechanism that directly shifts arm's control law with a bell-shaped speed). This trend seems to go in the opposite direction with respect to the most recent biological findings (e.g. [28]) that are accumulating evidence that brain regulates various aspects of motor behavior (e.g. motor planning and execution, processing of proprioceptive and visual information, space transformation) in a rather implicit, systemic, and emergent fashion.

Notwithstanding these interesting results, the model presented is only a first step of the broader mentioned research agenda as it has still many limits: (a) the model controls a simple two-segment arm having only two degrees of freedom; (b) the recruitment of motor neurons, abstracted in terms of desired EPs by the $\lambda$ model, should be substituted by a more realistic neural population process; (c) the encoding of joints' proprioception is done with neurons with Gaussian activations, while empirical evidence suggests they should have quasi-linear activations (cf. [21]); (d) the attentional processes regarding vision and proprioception are hardwired. These limits set important challenges for future work.

## REFERENCES


[1] J. Piaget, *The origins of intelligence in children*, I. U. Press, Ed., Newyork, 1952.

[2] C. von Hofsten, "Eye-hand coordination in newborns," *Developmental Psycology*, no. 18, pp. 450–461, 1982.

[3] M. Kuperstein, "Neural model of adaptive hand-eye coordination for single postures." *Science*, vol. 239, no. 4845, pp. 1308–1311, 1988.

[4] D. Bullock and S. Grossberg, "Vite and flete: neural modules for trajectory formation and postural control." North-Holland-Elsevier. Amsterdam., 1989, pp. 253–298.

[5] M. I. Jordan and D. E. Rumelhart, "Forward models: supervised learning with a distal teacher," *Cognitive science*, vol. 16, pp. 307–354, 1992.

[6] P. Morasso and V. Sanguineti, "Self organizing body schema fo motor planning," *Journal of Motor Behaviour*, vol. 27, no. 1, pp. 52–66, 1995.

[7] G. Asuni, G. Teti, C. Laschi, E. Guglielmelli, and P. Dario, "A robotic head neuro-controller based on biologically-inspired neural models," in *Proceedings of the 2005 IEEE International Conference on Robotics and Automation*, Barcelona, Spain, 2005, pp. 2362–2367.

[8] N. E. Berthier, M. T. Rosenstein, and A. G. Barto, "Approximate optimal control as a model for motor learning," *Psychological Review*, vol. Vol. 112, no. 2, pp. 329-346, 2005.

[9] J. Won and N. Hogan, "Stability properties of human reaching movements," *Exp Brain Res*, no. 107, pp. 125–136, 1995.

[10] J. Flanagan, D. Ostry, and A. Feldman, "Control of trajectory modifications in target-directed reaching." *J Mot Behav*, vol. 25, no. 3, pp. 140–152, 1993.

[11] K. N. An, F. C. Hui, B. F. Morrey, R. L. Linscheid, and E. Y. Chao, "Muscles across the elbow joint: a biomechanical analysis." *J Biomech*, vol. 14, no. 10, pp. 659–669, 1981.

[12] A. G. Feldman, "Once more on the equilibrium-point hypothesis (lambda model) for motor control." *J Mot Behav*, vol. 18, no. 1, pp. 17–54, 1986.

[13] R. Balasubramaniam and A. G. Feldman, "Guiding movements without redundancy problems," *Coordination dynamics: issues and trends. Springer*, pp. 155–176, 2004.

[14] T. J. Sejnowski, "Storing covariance with nonlinearly interacting neurons." *J Math Biol*, vol. 4, no. 4, pp. 303–321, 1977.

[15] W. Erlhagen and G. Schöner, "Dynamic field theory of movement preparation," *Psychological Review*, vol. 109, pp. 545–572, 2002.

[16] S. Ferraina, M. R. Garasto, A. Battaglia-Mayer, P. Ferraresi, P. B. Johnson, F. Lacquaniti, and R. Caminiti, "Visual control of hand-reaching movement: activity in parietal area 7m." *Eur J Neurosci*, vol. 9, no. 5, pp. 1090–1095, 1997.

[17] G. Bosco, R. E. Poppele, and J. Eian, "Reference frames for spinal proprioception limb endpoint based or joint-level based," *J Neurophysiol*, vol. 83, no. 5, pp. 2931–2945, 2000.

[18] T. Aflalo and M. Graziano, "Partial tuning of motor cortex neurons to final posture in a free moving paradigm," *PNAS*, vol. 103, no. 8, pp. 2909–2914, 2006.

[19] A. Pouget and P. E. Latham, "Population codes," in *The Handbook of Brain Theory and Neural Networks*, 2nd ed., M. A. Arbib, Ed. cambridge, MA, USA: The MIT Press, 2003.

[20] A. P. Georgopoulos, R. E. Kettner, and A. B. Schwartz, "Primate motor cortex and free arm movements to visual targets in three-dimensional space. ii. coding of the direction of movement by a neuronal population." *J Neurosci*, vol. 8, no. 8, pp. 2928–2937, 1988.

[21] M. Mascaro, A. Battaglia-Mayer, L. Nasi, D. J. Amit, and R. Caminiti, "The eye and the hand: neural mechanisms and network models for oculomanual coordination in parietal cortex." *Cereb Cortex*, vol. 13, no. 12, pp. 1276–1286, 2003.

[22] J. R. Flanagan and D. J. Ostry, "Trajectories of human multi-joint arm movements: Evidence of joint level planning," in *The First International Symposium on Experimental Robotics I*. London, UK: Springer-Verlag, 1990, pp. 594–613.

[23] A. V. Hill, "The heat of shortening and the dynamic constants of muscles." *Proocedings of the Royal Society*, pp. 136–195, 1938.

[24] J. J. Craig, *Introduction to Robotics: Mechanics and Control*. Boston, MA, USA: Addison-Wesley Longman Publishing Co., Inc., 1989.

[25] S. Amari, "Dynamics of pattern formation in lateral-inhibition type neural fields." *Biol Cybern*, vol. 27, no. 2, pp. 77–87, 1977.

[26] P. L. Gribble and D. J. Ostry, "Compensation for loads during arm movements using equilibrium-point control," *Exp. Brain Research*, no. 135, pp. 474–482, 2000.

[27] Y. Tanaka, T. Tsuji, V. Sanguineti, and P. G. Morasso, "Bio-mimetic trajectory generation using a neural time-base generator," *J. Robot. Syst.*, vol. 22, no. 11, pp. 625–637, 2005.

[28] P. Cisek, "Integrated neural processes for defining potential actions and deciding between them: a computational model." *J Neurosci*, vol. 26, no. 38, pp. 9761–9770, 2006.